ANALYSIS AND CORRELATIONS OF DIMENSIONLESS NUMBERS RELEVANT TO ORIFICES' CAVITATING FLOW

ABDUL-FATTAH MOHAMMED ALI[1,2]
AND MOHANAD JASIM MOHAMMED-RIDHA[1*]

[1]*Department of Environmental Engineering, University of Baghdad, Baghdad, Iraq*
[2]*Department of Oil and Gas Refining Engineering,*
Al-Farabi University College, Baghdad, Iraq

[*]*Corresponding author: muhannadenviro@coeng.uobaghdad.edu.iq*

ABSTRACT: The aim of this work was to establish a general design basis for pilot-scale units to treat textile dyeing wastewater containing recalcitrant organic chemicals by hydrodynamic cavitation (HC) using orifices of various geometries. Relevant tabulated data available in the literature were analyzed and correlated to obtain universal relationships to this end. In spite of extensive effort, most of the obtained correlations were system-specific, which still can be used for design using their respective orifice geometries as demonstrated. However, one salient general relationship links the pipe's dimensionless loss coefficient (K_{LP}) to the pipe's Reynolds number (Re_P), encompassing all data under consideration, which may serve as an additional design option to optimize such units. The implication of this relationship is a lower upstream pressure (P_1) value with an increase in pipe diameter while using the same specified orifice and achieving the same desired cavitation number (C_v). The ratio of P_1 value in the larger pipe to its value in the smaller pipe is a function of the smaller pipe diameter (D_S) to the larger pipe diameter (D_L) ratio: $(P_1 \text{ in } D_L) / (P_1 \text{ in } D_S) = (D_S/D_L)^{2.33}$. A lower P_1 value will increase the cavitation yield by decreasing the expended energy, especially if the required number of passes is large. Additionally, the variation of the orifices' hole loss coefficient (K_{Lh}) with the ratio of the holes area to the pipe cross-sectional area (A_h/A_p) for cavitating flow is compared with that for non-cavitating/incipient cavitation flow reported in the literature.

ABSTRAK: Tujuan kajian ini diadakan bagi mereka bentuk dasar umum unit skala-pandu bagi merawat pewarnaan air buangan tekstil yang mengandungi kimia organik rekalsitran daripada peronggaan hidrodinamik (HC) menggunakan orifis pelbagai geometri. Data berjadual berkaitan yang ada dalam kajian lepas dianalisa dan dikaitkan bagi mendapatkan kaitan universal hingga akhir. Walaupun pelbagai usaha telah dijalankan, banyak kaitan didapati mengguna pakai sistem-tertentu, di mana boleh digunakan bagi mereka cipta menggunakan geometri orifis yang ditunjukkan. Walau bagaimanapun, bagi menghubung kait pekali langsung tanpa dimensi (K_{LP}) kepada paip nombor Reynolds (Re_P), meliputi semua data di bawah pertimbangan, di mana membantu pilihan rekaan tambahan bagi mengoptimum unit tersebut. Implikasi hubungan ini adalah nilai tekanan hulu sungai bawah (P_1) dengan penambahan diameter paip dengan menggunakan orifis sama yang sebenar dan mendapati nombor peronggaan yang sama diingini (C_v). Nisbah nilai P_1 dalam paip besar kepada nilai paip kecil adalah berkadaran pada nisbah diameter paip kecil (D_S) kepada diameter paip besar (D_L):

$(P_1 \text{ dalam } D_L) / (P_1 \text{ in } D_S) = (D_S/D_L)^{2.33}$.

Nilai P_1 yang lebih kecil akan menambah jumlah peronggaan dengan pengurangan tenaga pengembangan, terutama jika nombor laluan yang diperlukan adalah besar. Tambahan, variasi orifis pekali langsung lubang (K_{Lh}) dengan nisbah keluasan lubang kepada ruang keratan-rentas paip (A_h/A_p) bagi alur rongga dibandingkan dengan bukan rongga / permulaan rongga alur telah dilapor dalam kajian

---

KEYWORDS: *hydrodynamic cavitation; orifice geometry; cavitation numbers; upstream pressure; loss coefficients*

1.   INTRODUCTION

Hydrodynamic cavitation (HC) is a well-established technique for a variety of applications including the treatment of wastewater containing pharmaceuticals [1], insecticides [2], phenolic compounds [3], and textile dyes [4-8]. HC is usually combined with the addition of an oxidizing agent (H_2O_2, NaOCl, etc.) or with acoustic cavitation to achieve an acceptable cavitation yield (CY) which is defined as the cavitation effect per unit energy supplied to the system.

Over the last two decades, many HC research studies have been published, some with detailed tabulated data. Their size-scale ranged from 1 L lab units to 50 L pilot ones. Various devices were used to induce HC in these units such as single-/multi-hole orifices, venturis, stator-rotor equipment, etc. The operational mode was batch-wise based either on fixed time or on a specified number of passes (turnovers) where the wastewater volume was recirculated many times through the HC device to achieve an acceptable CY. This could be hundreds of times, lasting over two hours depending on the system's flow rate (e.g. 260 passes lasting 130 min [7]).

Single-/multi-hole orifices as HC inducing devices are simpler to manufacture and install than other alternatives which explain their wide use in HC studies. Their hole size generally ranges from 1 to 5 mm with multi-hole counts of 8, 16, 20, 25, or 33, although some studies used sizes and counts outside these values. The pipes in which the aforementioned orifices were placed had inside diameters ranging from 4 to 53 mm.

The results obtained in all previously published HC studies were system-specific; a generalized or unifying approach were markedly lacking. Reviews stated only general trends based on the published works. Consequently, it is difficult to make practical use of available information, specifically a priori design of a functional wastewater-treating HC unit, save adopting a given system with all its particulars. The present work is an attempt at a unifying approach, relying entirely on tabulated data from a number of published research studies. The outcome of this endeavor was only partially productive as will be illustrated later by the obtained results. This research did not receive any specific grant from funding agencies in the public, commercial, or not-for-profit sectors.

2.   GEOMETRICAL DETAILS AND REFERENCES OF ORIFICES WHOSE HC PUBLISHED DATA WERE USED IN THIS WORK

Two categories of published data were excluded from the analysis and correlations performed in this study. The first concerned orifices with a hole size of one mm or less, whether single- or multi-hole ones. One mm holes or smaller are difficult/expensive to produce locally while ensuring their integrity (sharp edge, lack of burrs, etc.). The second category concerned a HC system in which the fully-recovered orifice's downstream pressure (P_2) was higher than atmospheric pressure (i.e. $P_2 >$ one atm. abs. or zero gage).

Data with $P_2 > 0$ gage did not match those with $P_2 \approx 0$ gage. Table 1 gives the details of the orifices whose HC data were used in this work along with their references.

The data of Testud et al. [10] and that of Mancuso et al. [7] were excluded due to P_2 values being greater than one atm. abs. as pointed out earlier. It should be stressed that all the HC data of the references cited in Table 1 are relevant to pilot-scale units with $P_2 \approx$ one atm. abs. Hence, all the obtained correlations of this work are only relevant to such systems.

Table 1: Geometrical details and references of orifices whose HC data
were employed in the analysis and correlations of this work.

Hole dia. [mm]	No. of holes	Pipe I.D [mm]	A_h/A_p	Reference
2	1	25.4	6.2×10^{-3}	[6]
2	1	25	6.4×10^{-3}	[9]
2	1	19	0.011	[8]
2	1	19	0.011	[17]
2	8	38	0.02216	[11]
2	8	38	0.02216	[4]
2	33	38	0.0914	[11]
2	33	38	0.0914	[4]
3	1	25.4	0.01395	[6]
3	1	19	0.02493	[17]
3	16	38	0.099723	[11]
3	16	38	0.099723	[4]
3	20	38	0.12465	[11]
3	20	38	0.12465	[4]
5	8	38	0.1385	[11]
5	8	38	0.1385	[4]

Notes: (i) A_h/A_p is the ratio of the total area of holes to the cross-sectional area of the pipe. (ii) Thicknesses of orifices in Table 1 references were not mentioned, apart from Pawar et al. [9] which was 4 mm leading to an aspect ratio of 2 (aspect ratio = orifice thickness/hole dia.). (iii) HC data listed in Table 1 references are extensive and can be referred to; they shall not be repeated in this article. (iv) A 4-mm single hole orifice datum from Madhu et al. [6] was excluded due to lack of 4-mm multi-hole data.

3. DIMENSIONLESS NUMBERS RELEVANT TO ORIFICE'S CAVITATING FLOW AND THEIR INTER-RELATIONSHIPS

3.1 Cavitation Number or Index

There are several definitions for this parameter, the two most widely used ones are C_v and σ (notations used are similar to those in the cited references) defined as follows:

$$C_v = (P_2 - P_v) / (0.5\, \rho_L\, u_o^2) \qquad \text{and} \qquad \sigma = (P_2 - P_v) / (P_1 - P_2)$$

where P_1, P_2 are the orifice's upstream and fully-recovered downstream pressures, respectively. P_v is the liquid-vapor pressure and ρ_L is its density, both at the operating temperature. u_o is the average liquid velocity at the orifice's hole (single hole or one hole in a multi-hole geometry).

Cavitating flow occurs when the value of C_v (or σ) is usually < 1, with an increase in cavitation intensity as the value of the index is lowered. Very low values of the index (<

0.1) may induce a regime called supercavitation which is counterproductive and should be avoided.

A modification of C_v (called C_v^{prime}) was introduced and used by Vichare et al. [11] and Sivakumar and Pandit [4] as a unifying approach for comparison of HC data of orifices with various multi-hole geometries. C_v^{prime} was defined as:

$$C_v^{prime} = C_v / [(\text{total perimeter of holes/perimeter of pipe})]$$

3.2 Flow Head Loss Coefficients and Reynolds Numbers

Two dimensionless flow head loss coefficients were used in this work. Their definitions are:

$$K_{Lh} = (P_1 - P_2) / (0.5\ \rho_L\ u_o^2) \qquad \text{and} \qquad K_{LP} = (P_1 - P_2) / (0.5\ \rho_L\ u_p^2)$$

K_{Lh} is based on the hole's dynamic pressure, whereas K_{LP} is based on the pipe's dynamic pressure with u_p being the average flow velocity in the pipe. Additionally, two Reynolds numbers were used, one based on the hole average velocity and the other one on the pipe average velocity:

$$Re_o = \rho_L\ u_o\ d_o / \mu_L \qquad \text{and} \qquad Re_p = \rho_L\ u_p\ D / \mu_L$$

where d_o and D are the hole diameter and the pipe inside diameter, respectively. μ_L is the liquid dynamic viscosity at the operating temperature.

3.3 Inter-relationships Among the Aforementioned Dimensionless Numbers

K_{Lh} is related to K_{LP} by (Maynes et al. [12]) Eq. (1):

$$K_{Lh} = (A_h/A_p)^2\ K_{LP} \tag{1}$$

and Re_p is related to Re_o by Eq. (2):

$$Re_P = Re_o\ [n\ (A_h/A_p)]^{0.5} \tag{2}$$

where n is the number of holes in the orifice (hole count) and A_h/A_p is the ratio of the total area of holes to the pipe cross-sectional area as pointed out earlier. Additionally, σ is related to C_v by Eq. (3):

$$\sigma = C_v / K_{Lh} \tag{3}$$

The relationships represented by Eqs. (1) to (3) can be easily obtained by considering the given definitions of the dimensionless numbers involved.

The orifices' HC tabulated data of Table 1 references constituted experimental values of P_1, C_v, u_o, A_h/A_p, flow rate, and temperature. P_2 values were either given or calculated using the above relationships, where it was confirmed that its value was virtually one atm. abs. in all cases. Eq. (3) was used to calculate the corresponding σ values.

4. SPECIFIC CORRELATIONS OF ORIFICES' CAVITATING FLOW DIMENSIONLESS NUMBERS AND THEIR UTILITY IN DESIGN

Cavitating flow is a complex phenomenon that is still not-well understood and whose theoretical basis has not been fully established. Consequently, an empirical approach is usually adopted (Burzio et al. [18]). Accordingly, Eqs. (4) to (18) are empirical; only

characterized by values of the determination coefficient $R^2 > 0.9$. Furthermore, the data upon which they are based (Table 1) lacked standard deviation bounds which compromise their accuracy. Notwithstanding these limitations, the equations are of use in a priori design of HC pilot-scale units (as elucidated in section 4.5) where plus or minus 5% off specification is usually acceptable.

Table 2 expounds the types of correlations employed and equations designation as related to five orifice geometries. Two other geometries pertaining to the 2mm and 3mm single hole orifices were excluded from the said correlations due to their trend-lacking scattered data. Additionally, Eqs. 13 to 15 were also excluded from Table 2 because they represent a test for C_v^{prime} as a unifying parameter.

Table 2: Types of correlation, equations designation and corresponding orifice geometries

Correlation type	2mm-8h	2mm-33h	3mm-16h	3mm-20h	5mm-8h
K_{Lh} vs. Re_o	Eq. (4)	----------	----------	Eq. (5)	---------
K_{Lh} vs. C_v	Eq. (6)	----------	----------	Eq. (7)	---------
σ vs. Re_o	Eq. (8)	Eq. (9)	----------	----------	Eq. (10)
σ vs. C_v	Eq. (11)	Eq. (12)	Eq. (16)	Eq. (17)	Eq. (18)

Notes: (i) In the design procedure, the value of C_v is initially assumed depending on the application (see sec. 4.5) which leads to the calculation of Re_o. (ii) For a selected geometry, K_{Lh} or σ is then determined from an appropriate equation(s) leading to the value of P_1 (a prime design parameter). (iii) There are 4 choices to accomplish note (ii) for 2mm-8holes, 3 choices for 3mm-20holes, 2 choices for either 2mm-33holes or 5mm-8holes, but only one choice for the 3mm-16holes geometry.

4.1 K_{Lh} vs Re_o Correlations

For this category, only two specific correlations were obtained as shown in Fig. 1.
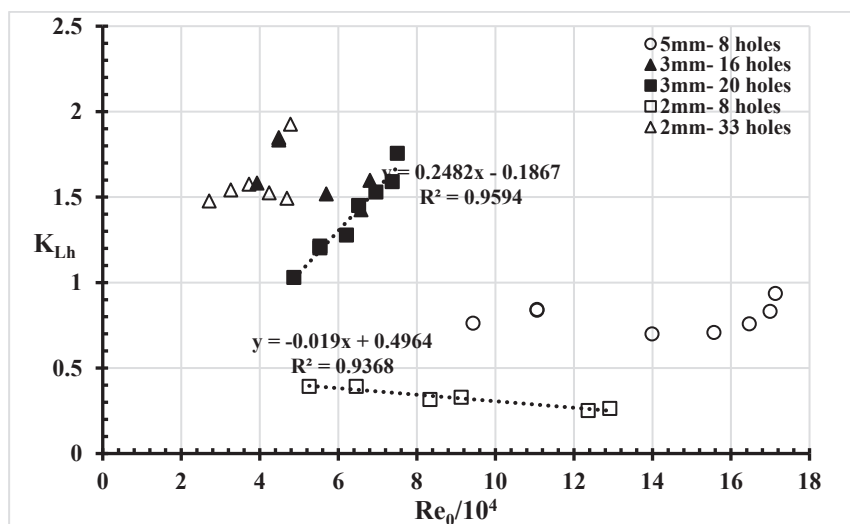

Fig. 1: K_{Lh} vs $Re_o/10^4$.

$$K_{Lh} = 0.4964 - 0.019 \,(Re_o/10^4) \qquad (4)$$

(2mm-8holes, $5 \leq Re_o/10^4 \leq 13$, $R^2 = 0.9368$)

$$K_{Lh} = 0.2482 \,(Re_o/10^4) - 0.1876 \qquad (5)$$

(3mm-20holes, $4.5 \leq Re_o/10^4 \leq 8$, $R^2 = 0.9594$)

The trends of Eqs. (4) and (5) are opposite to one another. The 2mm-8holes K_{Lh} decreases with increasing Re_o (A_h/A_p = 2.2%) whereas the 3mm-20holes K_{Lh} increases (A_h/A_p = 12%). Also shown in Fig. 1 are the data of the 2mm-33holes (A_h/A_p = 9.1%) and the 5mm-8holes (A_h/A_p = 13.85%). The former reflects an increasing-decreasing trend, whilst the latter depicts a clearly non-linear increasing trend for $Re_o > 16 \times 10^4$. Maynes et al. [12] had shown an increasing K_{Lh} trend with increasing u_o for two multi-hole orifices with A_h/A_p values of 22% and 44% which they attributed to cavitating flow, since according to their results for non-cavitating flow K_{Lh} was constant and independent of u_o. Any explanation for the above observations would be premature at this stage.

4.2 K_{Lh} vs C_v Correlations

The following specific correlations were obtained for this category.

$$K_{Lh} = 1.0192\, C_v + 0.2095 \tag{6}$$

(2mm-8holes, $0.045 \le C_v \le 0.56$, $R^2 = 0.9956$, Fig. 2)

$$K_{Lh} = 0.862\, C_v^{-0.567} \tag{7}$$

(3mm-20holes, $0.3 \le C_v \le 0.75$, $R^2 = 0.9681$, Fig. 3)

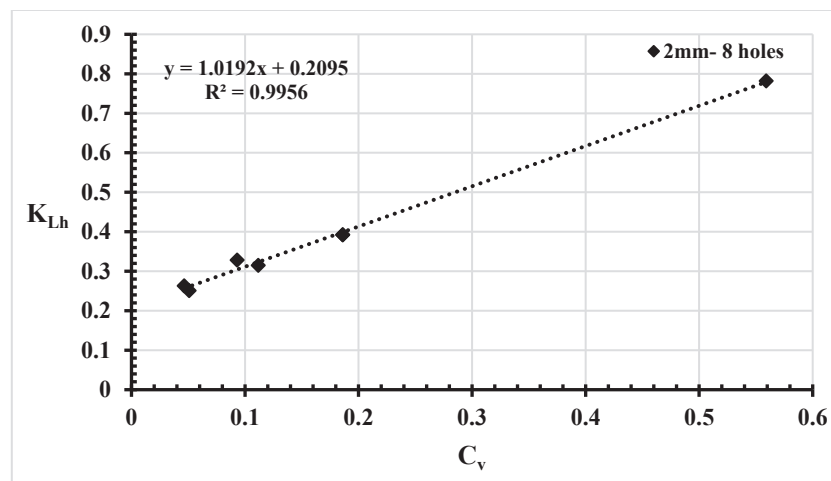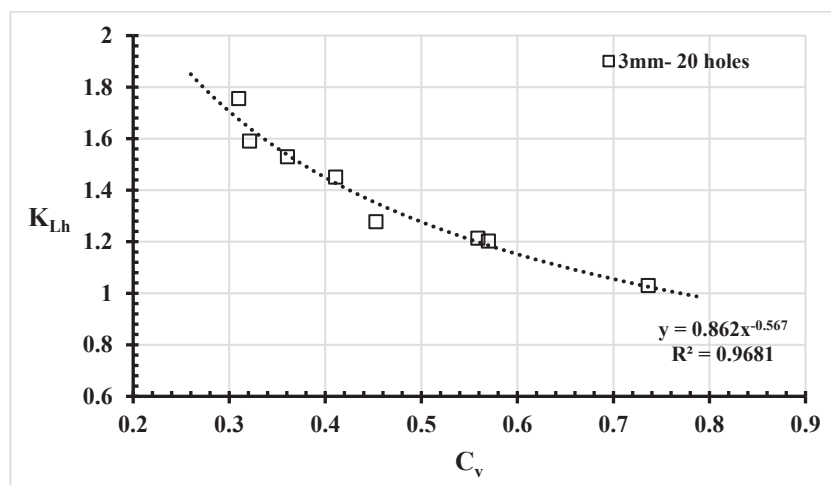Fig. 2: K_{Lh} vs C_v 2mm-8holes.

Fig. 3: K_{Lh} vs C_v 3mm-20holes.

The trends represented by Eqs. (6) and (7) are opposite to one another. For each geometry, the above trend is the reverse of its K_{Lh} vs Re_o trend [Eqs. (4) and (5)]. Hence, K_{Lh} increases with increasing C_v for the geometry of the 2mm-8 holes [Eq. (6)] whereas it decreases for the 3mm-20holes one [Eq. (7)].

4.3 σ vs Re₀ Correlations

For this category, the following specific relationships were obtained:

$$\sigma = 0.8139 - 0.0159 \, (Re_o/10^4) \tag{8}$$

(2mm-8holes, $3.7 \le Re_o/10^4 \le 13$, $R^2 = 0.9095$, Fig. 4)

$$\sigma = 1.0317 - 0.1757 \, (Re_o/10^4) \tag{9}$$

(2mm-33holes, $3 \le Re_o/10^4 \le 5$, $R^2 = 0.9644$, Fig. 4)

$$\sigma = 65.504 \, (Re_o/10^4)^{-2.027} \tag{10}$$

(5mm-8holes, $9 \le Re_o/10^4 \le 17.5$, $R^2 = 0.9559$, Fig. 5)

Equations (8) to (10) indicate a decreasing trend of σ with increasing Re_o for different geometries. This was expected since higher Re_o values imply higher P_1 values making σ smaller since P_2 and P_v are fixed, $[\sigma = (P_2 - P_v)/(P_1 - P_2)]$.
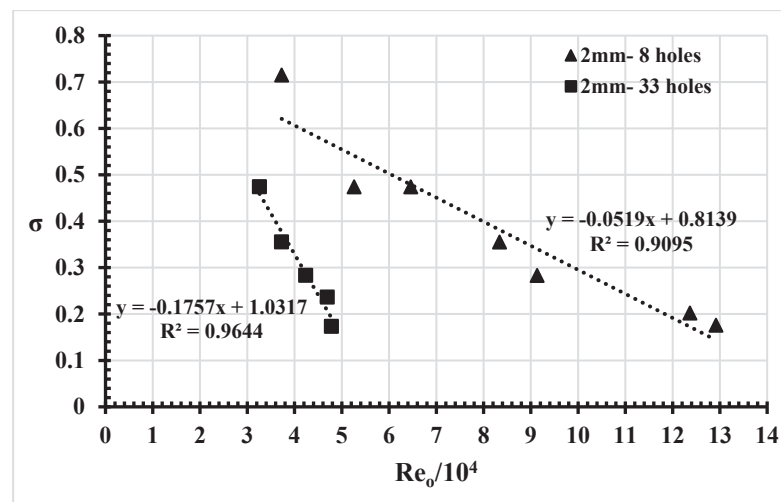

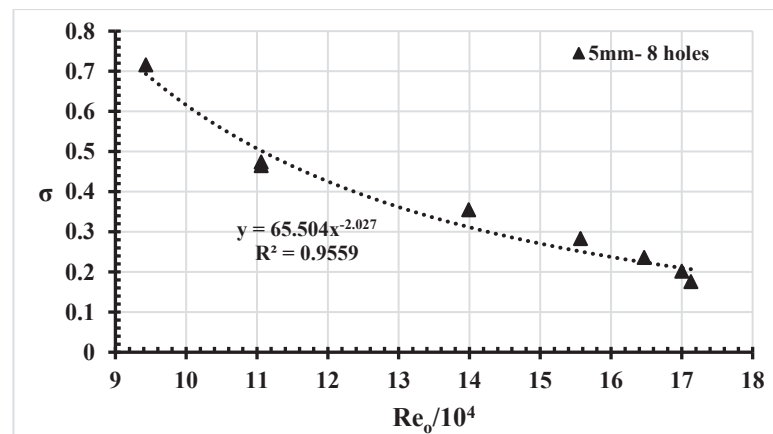Fig. 4: σ vs $Re_o/10^4$ for 2 mm-8, 33holes.

Fig. 5: σ vs $Re_o/10^4$ for 5mm-8holes.

4.4 σ vs C_v or C_v^{prime} Correlations

Specific correlations linking the two most widely-used definitions of cavitation number were as follows:

$$\sigma = 1.016\ C_v^{0.5509} \tag{11}$$

(2mm-8 oles, $0.045 \le C_v \le 0.56$, $R^2 = 0.9647$, Fig. 6)

$$\sigma = 0.6848\ C_v - 0.0262 \tag{12}$$

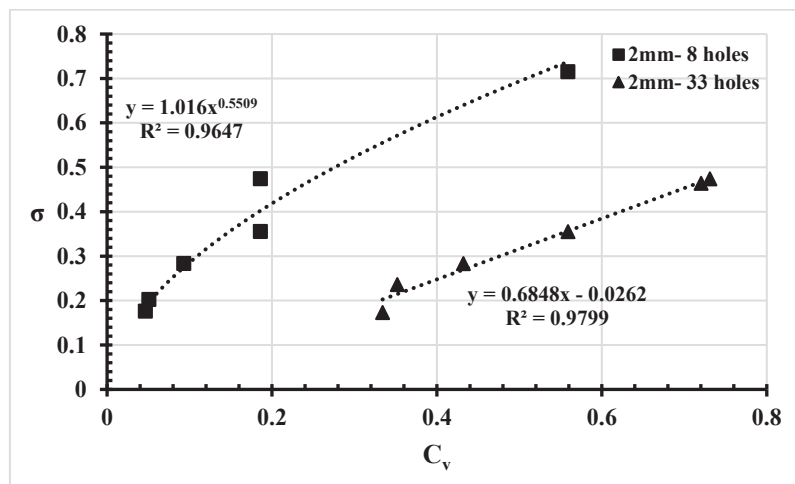(2mm-33 holes, $0.35 \le C_v \le 0.75$, $R^2 = 0.9799$, Fig. 6)

Fig. 6: σ vs Cv for 2mm-8, 33holes.

The two geometries of Eqs. (11) and (12) were combined by a single σ vs C_v^{prime} correlation:

$$\sigma = 0.9478\ C_v^{prime} + 0.0593 \tag{13}$$

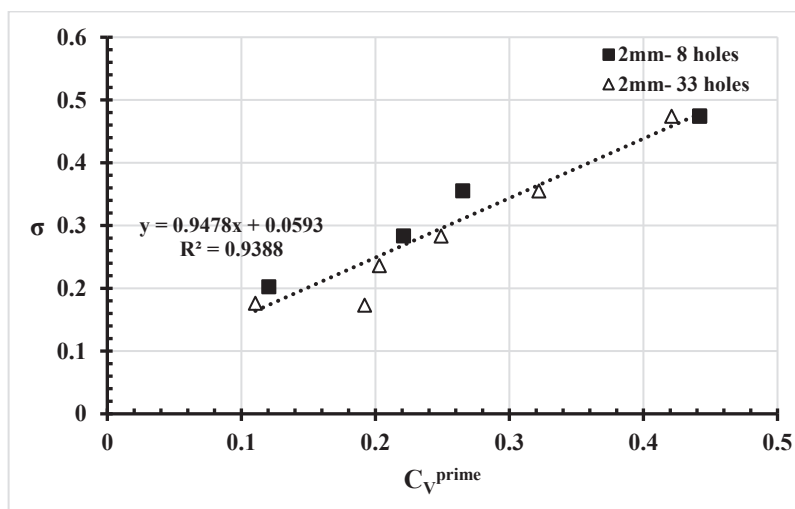(2mm-8, 33 holes, $0.1 \le C_v^{prime} \le 0.45$, $R^2 = 0.9388$, Fig. 7)

Fig. 7: σ vs C_v^{prime} for combined 2mm-8, 33holes.

Equation (13) is the only case where C_v^{prime} acted as a unifying parameter. Consequently, two additional σ vs C_v specific relationships were deduced for imaginary geometries of 2mm-16holes and 2mm-20holes:

$$\sigma = 1.1255\ C_v + 0.0593 \tag{14}$$

$$(\text{2mm-16holes},\ 0.0842 \leq C_v \leq 0.379)$$

$$\sigma = 0.9004\ C_v + 0.0593 \tag{15}$$

$$(\text{2mm-20holes},\ 0.1053 \leq C_v \leq 0.477)$$

Additionally, the following specific σ vs C_v correlations were obtained:

$$\sigma = 0.5995\ C_v - 0.0081 \tag{16}$$

$$(\text{3mm-16holes},\ 0.37 \leq C_v \leq 1.15,\ R^2 = 0.9602,\ \text{Fig. 8})$$

$$\sigma = 1.2227\ C_v - 0.206 \tag{17}$$

$$(\text{3mm-20holes},\ 0.3 \leq C_v \leq 0.75,\ R^2 = 0.9936,\ \text{Fig. 8})$$

$$\sigma = 1.2676\ C_v \tag{18}$$

$$(\text{5mm-8holes},\ 0.15 \leq C_v \leq 0.55,\ R^2 = 0.9732,\ \text{Fig. 9})$$

Equations (11) to (18) reflect a trend of increasing σ with increasing C_v for the various orifice geometries. This trend was also expected since an increase in C_v value means a lower u_o value which entails a lower P_1 value leading to an increase in the value of σ.
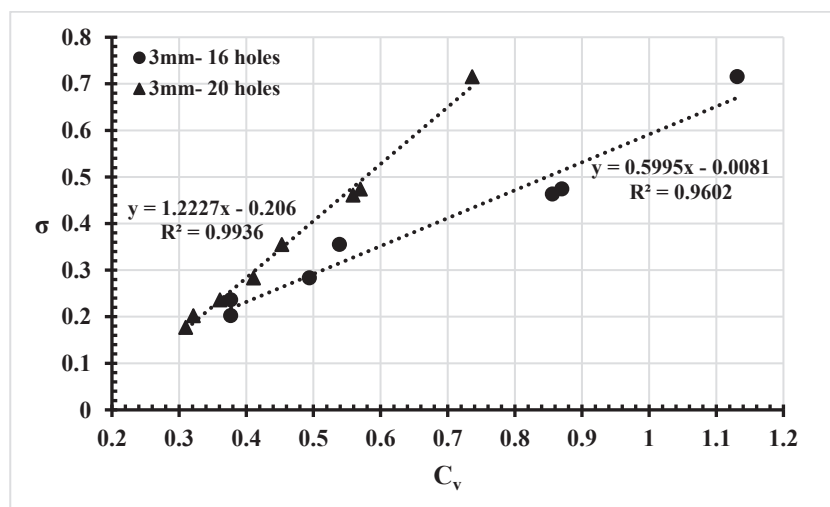

Fig. 8: σ vs Cv for 3mm-16, 20holes.

Yan and Thorpe [13] derived a theoretical equation linking σ to C_v for a single hole orifice. Their relationship included the orifice's discharge coefficient C_d , its contraction coefficient C_c , and A_h/A_p . It was not possible to compare Eqs. (11) to (18) with their equation because C_d and C_c were not given for the orifices under consideration in this work. Estimating the values of C_d and C_c from correlations available in the literature would be uncertain since they are related to the aspect ratio, which is also missing for all the multi-hole orifices of Table 1.
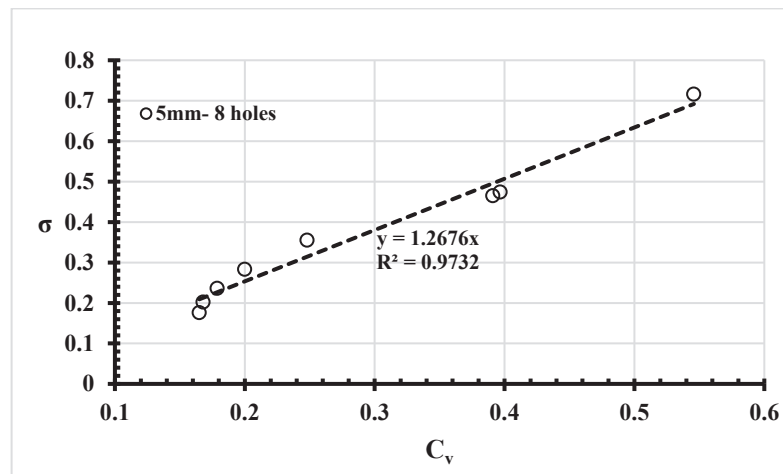
Fig. 9: σ vs Cv for 5 mm-8holes.

4.5   Outline of a Priori Design Procedure Utilising the Specific Correlations

(a) Initially an appropriate C_v value for the intended application is chosen, e.g. for wastewater containing bio-refractory organic dyes, a suitable range is $0.2 \leq C_v \leq 0.4$ (Rajoriya et al. [19])

(b) Since $C_v = (P_2 - P_v)/(0.5 \, \rho_L \, u_o^2)$, u_o can be determined after an operating temperature is set, fixing the values of P_v, ρ_L, and μ_L. Hence the value of Re_o can be established.

(c) After selecting an orifice geometry, one or more correlation may be used to calculate either K_{Lh} or σ from which the value of P_1 can be determined. This P_1 value is based on 38 mm (1.5 inch) pipe diameter (see Table 1).

(d) The 38mm-based P_1 value can be lowered by specifying a larger pipe diameter, e.g. 53mm (2 inch) according to the findings of sec. 5 below. $(P_1 - P_2)$ represents the main pressure drop of the system whose volumetric flow rate (Q) can be calculated from the value of u_o and the selected geometry leading to the estimation of the system's total pressure drop (ΔP).

(e) A centrifugal pump whose best efficieny point (BEP) matches the system's Q-ΔP point should be employed. Conversely, if a pump is already available, an appropriate C_v value, the ensuing P_1 and reduced P_1 values, and selected geometry should be manipulated to achieve the pump's BEP-system's Q-ΔP match.

5.   GENERAL K_{LP} vs Re_P CORRELATION AND ITS IMPLICATIONS

Figure 10 shows a plot of K_{LP} vs. Re_p for all the HC data of the orifices listed in Table 1, including the single hole data which were excluded from the specific correlations of sec. 4 due to their trend-lacking scatter. It is noteworthy that four pipe sizes are included in Fig. 10 with a range of $19 \leq I.D. \leq 38$ mm, which is in contrast with the specific correlations where only a single pipe size of I.D = 38 mm was involved. The unifying characteristic of K_{LP} vs Re_p is clear, resulting in the following general correlation Eq. (19):

$$K_{LP} = 4228.5 \, (Re_p/10^4)^{-1.6707} \qquad\qquad (19)$$

$$\{(Re_p/10^4) \leq 18, R^2 = 0.9353\}$$

Retrieving the definitions of $K_{LP} = (P_1 - P_2)/(0.5\ \rho_L\ u_p^2)$ and $Re_p = (\rho_L\ u_p\ D)/\mu_L$, Fig. 10 indicates that increasing Re_p by increasing u_p, which can only come about by increasing P_1 reduces K_{LP} in a nearly exponential decay manner. If the definitions of K_{LP} and Re_p are substituted into Eq. (19) and noting that $(P_1 - P_2)$ may be replaced by P_1 as gage pressure, then Eq. (19) can take the following form:

$$P_1 = 1.0185 \times 10^5\ \rho_L^{-0.6707}\ \mu_L^{1.6707}\ u_p^{0.3293}\ D^{-1.6707} \qquad (20)$$
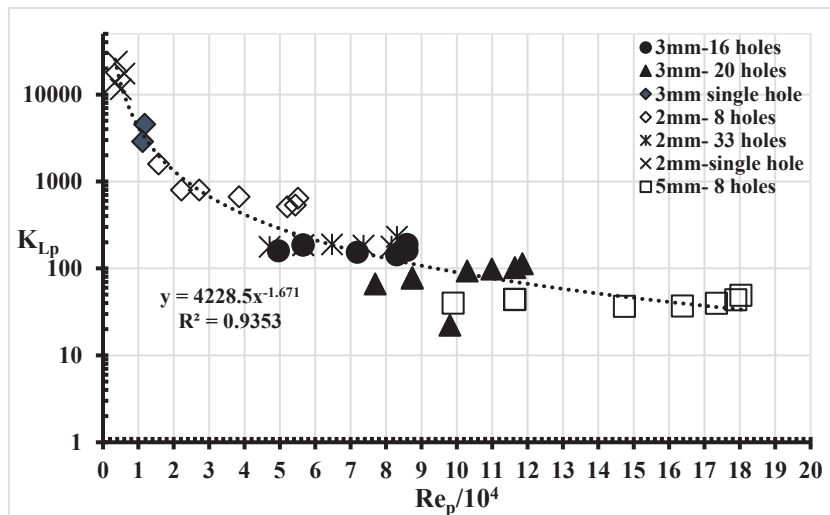
where P_1 has units of bar gage.

Fig. 10: K_{Lp} vs $Re_{ep}/10^4$ for all single and multi-hole orifices.

If for a specific orifice geometry and a desired C_v value, two pipes are considered (in which the specified orifice is to be installed in one of them) one pipe with a smaller inside diameter D_S and the other with a larger inside diameter D_L, then the application of Eq. (20) and the equation of continuity (conservation of mass flow rate) for the two pipes will result in the following ratio Eq. (21): (see Appendix A),

$$(P_1 \text{ in } D_L \text{ pipe } / P_1 \text{ in } D_S \text{ pipe}) = (D_S / D_L)^{2.33} \qquad (21)$$

Hence, a lower value of P_1 is required to obtain the desired C_v value by installing the specified orifice in a larger I.D pipe compared to a smaller I.D. pipe. It is emphasized that this result is limited to the applicability range of Eq. (19) and the data upon which it is based.

An additional advantage of using a relatively larger inside diameter pipe is the lower pressure drop in the system, apart from the orifice's pressure drop $(P_1 - P_2)$, especially when the required number of passes is large. This will have a positive effect on the expended energy and consequently on the cavitation yield.

A possible drawback of lowering P_1 value by using a larger inside diameter pipe is the ensuing decrease in the value of the cavity collapse pressure given by the following empirical correlation [14-16] Eq. (22).

$$P_{collapse} = 7527\ [100\ (A_h/A_p)]^{-2.55}\ P_1^{2.46}\ R_o^{-0.8}\ d_o^{2.37} \qquad (22)$$

which is related to the cavitation yield by Eq. (23):

$$CY = K \ (\ P_{collapse} \ )^{\mathbf{W}} \tag{23}$$

where R_o is the initial cavity size, K and w are constants whose values depend on the system's particulars (device geometry, operating parameters, type of reaction). However, the possible negative effect of lower P_1 value may be partially or totally offset by the decrease in the value of A_h/A_p with a larger inside diameter pipe and/or the value of w being positive or negative.

Applying Eq. (22) with D_S or D_L leads to:

$$(P_{collapse} \text{ in } D_L \text{ pipe})/(P_{collapse} \text{ in } D_S \text{ pipe}) = (D_S/ \ D_L)^{\mathbf{0.632}} \tag{24}$$

6. COMPARISON WITH FINDINGS OF MAYNES et al. [12]

Maynes et al. [12] showed a graphical representation of K_{Lh} vs A_h/A_p in which data points pertaining to 16 multi-hole orifices of their work plus data points from three references were all bounded by two theoretical models, namely Eqs. (25) and (26):

$$(K_{Lh})_{Detached} \ = [C_c^{\mathbf{-1}} - (A_h/A_p)]^{\mathbf{2}} \tag{25}$$

$$(K_{Lh})_{Attached} \ = 2 \ [1- (A_h/A_p) - C_c^{\mathbf{-1}}] + C_c^{\mathbf{-2}} + (A_h/A_p)^{\mathbf{2}} \tag{26}$$

These models were derived by Testud et al. [10] for single hole orifice using Bernoulli's principle and conservation of momentum for non-cavitating flow. Eq. (25) is relevant to a thin orifice where the flow does not reattach within the hole, whereas Eq. (26) is for a thick orifice where the flow is reattached. C_c value for Eq. (25) was determined from Busemann theoretical relation cited by Maynes et al. [12] (a function of A_h/A_p) whilst for Eq. (26) it was given a fixed value of 0.75. Maynes et al. emphasized that all the shown data were non-cavitating/incipient-cavitation points. However, the two included points from Testud et al. are developed cavitation results (one for a single hole and the other for multi-hole orifices with aspect ratios of 0.64 and 4.67, respectively).
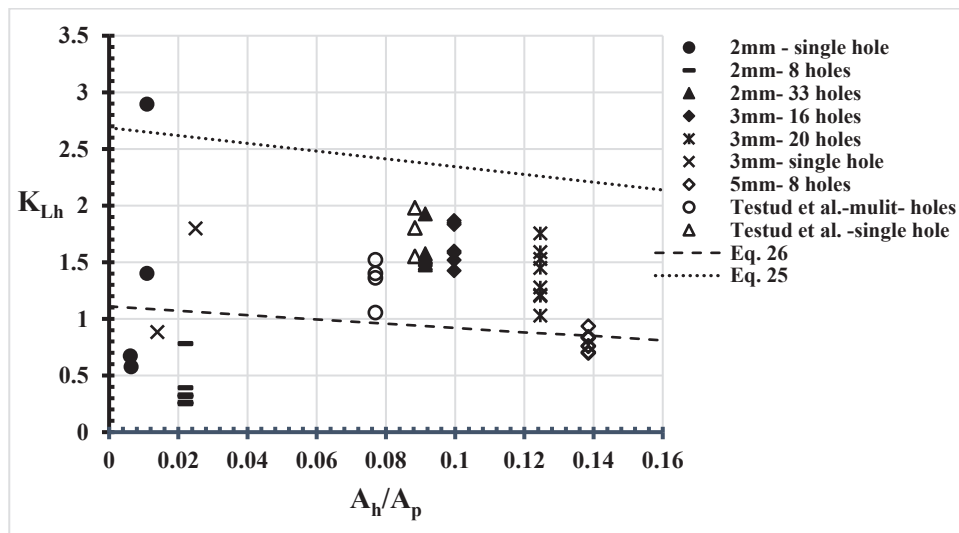

Fig. 11: K_{Lh} vs A_h/A_p for all single and multi-hole orifices.

Figure 11 is a reproduction of Maynes et al. [12] presentation where the upper line represents Eq. (25) and the lower line Eq. (26). The plotted points are all the data of Table

1 plus all the developed cavitation results of Testud et al. [10]. Hence, all the points in Fig. 11 are cavitating flow results. The 2 mm and 3 mm single hole points having very small A_h/A_p values lie mainly below or in-between the bounds representing Eqs. (25) and (26). As for the multi-hole orifices data and that of Testud et al. [10], there seems to be a trend with increasing value of A_h/A_p starting below the lower bound (2mm-8holes), then in-between the two bounds and finally back to the lower bound (5mm-8holes). It is therefore concluded that results falling in-between these two bounds are not necessarily non-cavitating/incipient cavitation data and could very well be developed cavitation results.

7. CONCLUSIONS

Correlations represented by Eqs. (4) to (12) and Eqs. (16) to (18), although specific to their respective orifice geometries, can be used to design and/or predict the performance of pilot-scale HC units for wastewater treatment. This includes a priori determination of P_1 and $(P_1 - P_2)$ values for the desired C_v value using a specific orifice geometry. Furthermore, they can be used to design systems to suit available pumps in order to obtain operating points at or very close to the pump's best efficiency points. This will increase the cavitation yield by lowering the value of the expended energy.

The pipe's loss coefficient K_{LP} and the pipe's Reynolds number Re_p were the only dimensionless parameters that unified all the HC data of orifices of various geometries and pipe sizes in a single general correlation with $R^2 = 0.9353$. This resultant correlation, Eq. (19), implies that for the same specified orifice geometry and desired C_v value, using a relatively larger pipe inside diameter entails a reduction in the value of the required upstream pressure P_1. The ratio of P_1 value in the larger pipe to its value in the smaller pipe is a function of the ratio of the smaller pipe diameter (D_S) to the larger pipe diameter (D_L): $(P_1 \text{ in } D_L) / (P_1 \text{ in } D_S) = (D_S / D_L)^{2.33}$. A lower P_1 value will increase the cavitation yield by decreasing the expended energy especially if the number of passes is large. However, a lower P_1 value will also decrease the value of the cavity collapse pressure which may affect the cavitation yield negatively, positively, or not at all depending on A_h/A_p variation and on constants whose values are system-specific.

The findings of Maynes et al. [12] that non-cavitating/incipient cavitation orifices' K_{Lh} vs A_h/A_p data fall in-between two theoretical models, Eqs. (25) and (26), are not exclusive. Orifices' cavitating flow results may also behave likewise, but with a discernible trend.

REFERENCES

[1] Braeutigam P, Franke M, Schneider RJ, Lehmann A, Stolle A, Ondruschka B. (2012) Degradation of carbamazepine in environmentally relevant concentrations in water by hydrodynamic-acoustic cavitation (HAC). Water Res., 46:2469-2477.

[2] Patil PN, Bote SD, Gogate PR. (2014) Degradation of imidacloprid using combined advanced oxidation processes based on hydrodynamic cavitation. Ultrason. Sonochem., 21:1770-1777.

[3] Pradham AA, Gogate PR. (2010) Removal of p-nitrophenol using hydrodynamic cavitation and Fenton chemistry at pilot scale operation, Chem. Eng. J., 156:77-82.

[4] Sivakumar M, Pandit AB. (2002) Wastewater treatment: a novel energy efficient hydrodynamic cavitational technique. Ultrason. Sonochem., 9:123-131.

[5] Saharan VK, Pandit AB, Kumar PSS, Anandan S. (2012) Hydrodynamic Cavitation as an Advanced Oxidation Technique for the Degradation of Acid Red 88 Dye. Ind. Eng. Chem. Res., 51:1981-1989.

[6]   Madhu GM, Thomas A, Deepak S, Preetham HS, Rajanandam KS. (2015) Escalation of degradation of malachite green and methyl violet using hydrodynamic cavitation using different orifice geometry. Int. J. Env. Sci., 5(4):880.

[7]   Mancuso G, Langone M, Laezza M, Andreottola G. (2016) Decolourization of Rhodamine B: A swirling jet-induced cavitation combined with NaOCl. Ulatrason. Sonochem., 32:18-30.

[8]   Rajoriya S, Bargole S, Saharan VK. (2017) Degradation of reactive blue 13 using hydrodynamic cavitation: Effect of geometrical parameters and different oxidizing additives. Ultrason. Sonochem., 37:192-202, DOI:http://doi.org/10.1016/j.ultsonch.2017.01.005

[9]   Pawar SK, Mahulkar AV, Pandit AB, Roy K, Moholkar VS. (2017) Sonochemical Effect Induced by Hydrodynamic Cavitation: Comparison of Venturi/Orifice Flow Geometries. AIChE Journal, 63(10):4705-4716.

[10] Testud P, Moussou P, Hirschberg A, Auregan Y. (2007) Noise generated by cavitating single-hole and multi-hole orifices in a water pipe. J. Fluids and Structures, 23:163-189.

[11] Vichare N P, Gogate PR, Pandit AB. (2013) Optimization of hydrodynamic cavitation using a model reaction. Chemical Engineering Technology, 23:683-690.

[12] Maynes D, Holt GJ, Blotter J. (2013) Cavitation Inception and Head loss Due to Liquid Flow Through Perforated Plates of Varying Thickness. J. Fluids Eng., 135: 031302-1—031302-11.

[13] Yan Y, Thorpe RB. (1990) Flow Regime Transitions Due to Cavitation in the Flow Through an Orifice. Int. J. Multiphase Flow, 16 (6):1023-1045.

[14] Gogate PR, Pandit AB. (2000) Engineering Design Methods for Cavitation Reactors II: Hydrodynamic Cavitation. AIChE J., 46 (8):1641-1649.

[15] Gogate PR, Shirganokar IZ, Sivakumar M, Senthilkumar P, Vichare NP, Pandit AB. (2001) Cavitation Reactors: Efficiency Assessment Using a Model Reaction. AIChE J., 47 (11):2526-2538.

[16] Gogate PR, Pandit AB. (2005) A review and assessment on hydrodynamic cavitation as a technology for the future. Ultrason. Sonochem., 12:21-27.

[17] Carpenter J, Badve M, Rajoriya S, George S, Saharan VK, Pandit AB. (2017) Hydrodynamic cavitation: An emerging technology for the intensification of various chemical and physical processes in a chemical process industry. Reviews in Chemical Engineering, 33(5):433-468. https://doi.org/10.1515/revce-2016-0032.

[18] Burzio E, Bersani F, Caridi GCA, Vesipa R, Ridolfi L, Manes C. (2020) Water disinfection by orifice-induced hydrodynamic cavitation. Ultrasonics-Sonochemistry, 60, 104740: 1-13.

[19] Rajoriya S, Carpenter J, Saharan VK, Pandit AB. (2016) Hydrodynamic cavitation: an advanced oxidation process for the degradation of bio-refractory pollutants. Rev. Chem. Eng., 32: 379-411.

APPENDIX A

The mass flow rate and volumetric flow rate (Q) will be the same in both D_L and D_S pipes, therefore,

$$P_1 \text{ in } D_L \text{ pipe} = 1.0185 \times 10^5 \, \rho_L^{-0.6707} \, \mu_L^{1.6707} \, (4Q/\pi D_L^2)^{0.3293} \, D_L^{-1.6707}$$

$$P_1 \text{ in } D_S \text{ pipe} = 1.0185 \times 10^5 \, \rho_L^{-0.6707} \, \mu_L^{1.6707} \, (4Q/\pi D_S^2)^{0.3293} \, D_S^{-1.6707}$$

Dividing: $(P_1 \text{ in } D_L \text{ pipe} / P_1 \text{ in } D_S \text{ pipe}) = (D_L^{-0.6586} \, D_L^{-1.6707}) / (D_S^{-0.6586} \, D_S^{-1.6707})$

$$= D_L^{-2.33} / D_S^{-2.33} = (D_S / D_L)^{2.33}$$